SECURITY CLASSIFICATION OF THIS PAGE

RT DOCUMENTATION PAGE DTIC FILE COPY

1a. R
1
2a. SI

AD-A197 423

1b RESTRICTIVE MARKINGS	
2b. DECLASSIFICATION / DOWNGRADING SCHEDULE	3. DISTRIBUTION / AVAILABILITY OF REPORT Approved for public release and sale. Distribution unlimited.
4. PERFORMING ORGANIZATION REPORT NUMBER(S) ONR Technical Report No. 8	5. MONITORING ORGANIZATION REPORT NUMBER(S)
6a. NAME OF PERFORMING ORGANIZATION University of Utah 6b. OFFICE SYMBOL (If applicable)	7a NAME OF MONITORING ORGANIZATION
6c. ADDRESS (City, State, and ZIP Code) Department of Chemistry Henry Eyring Building Salt Lake City, UT 84112	7b ADDRESS (City, State, and ZIP Code)
8a. NAME OF FUNDING / SPONSORING ORGANIZATION Office of Naval Research 8b. OFFICE SYMBOL (If applicable)	9. PROCUREMENT INSTRUMENT IDENTIFICATION NUMBER N00014-85-K-0712
8c. ADDRESS (City, State, and ZIP Code) Chemistry Program, Code 1113 800 N. Quincy Street Arlington, VA 22217	10 SOURCE OF FUNDING NUMBERS PROGRAM ELEMENT NO. / PROJECT NO. / TASK NO. / WORK UNIT ACCESSION NO

11. TITLE (Include Security Classification)
Total Internal Reflection Fluorescence for Adsorbed Probe Molecule Studies of Liquid/Solid Interfacial Environments

12. PERSONAL AUTHOR(S)
K. C. Hartner, J. W. Carr, and J. M. Harris

13a. TYPE OF REPORT	13b TIME COVERED	14. DATE OF REPORT (Year, Month, Day)	15. PAGE COUNT
Technical	FROM 9/87 TO 7/88	July 15, 1988	25

16. SUPPLEMENTARY NOTATION

17 COSATI CODES			18. SUBJECT TERMS (Continue on reverse if necessary and identify by block number)
FIELD	GROUP	SUB-GROUP	Fluorescence spectroscopy of liquid/solid interfaces, chemical effects of surface geometry

19. ABSTRACT (Continue on reverse if necessary and identify by block number)

Attached.

DTIC ELECTED JUL 27 1988 S D H

20 DISTRIBUTION / AVAILABILITY OF ABSTRACT ☒ UNCLASSIFIED/UNLIMITED ☐ SAME AS RPT ☐ DTIC USERS	21 ABSTRACT SECURITY CLASSIFICATION Unclassified
22a NAME OF RESPONSIBLE INDIVIDUAL	22b TELEPHONE (Include Area Code) / 22c OFFICE SYMBOL

DD FORM 1473, 84 MAR 83 APR edition may be used until exhausted
All other editions are obsolete

SECURITY CLASSIFICATION OF THIS PAGE

OFFICE OF NAVAL RESEARCH

Contract N00014-85-K-0712

R&T Code 413a001---01
Replaces Old Task #056-123

Technical Report No. 8

Total Internal Reflection Fluorescence for Adsorbed Probe Molecule Studies of Liquid/Solid Interfacial Environments

Prepared for publication in Applied Spectroscopy

by

K. C. Hartner, J. W. Carr and J. M. Harris

Department of Chemistry
University of Utah
Salt Lake City, UT 84112

July 15, 1988

TOTAL INTERNAL REFLECTION FLUORESCENCE FOR ADSORBED PROBE MOLECULE STUDIES OF LIQUID/SOLID INTERFACIAL ENVIRONMENTS

K. C. Hartner, J. W. Carr+, and J. M. Harris*
Department of Chemistry
University of Utah
Salt Lake City, UT 84112

Abstract

Total internal reflection fluorescence (TIRF) is developed as a surface selective method to allow the environment of a liquid-solid interface to be probed by fluorescent molecules which are adsorbed from solution. The method has been used to detect pyrene sorbed to an octadecylsilane derivatized, fused silica plate and resolve its spectral emission so that vibronic intensity ratios can be calculated and the surface environment characterized. Adsorption equilibria of the fluorescent probe to the surface and the depth of penetration of the evanescent excitation beam provide the basis for predicting interference from probe molecules in the solution phase. These predictions were validated by replacing the solution overlaying the alkylated silica interface with saturated vapor and comparing the apparent surface environments.

Index Headings: Fluorescence Spectroscopy; Total Internal Reflection Fluorescence (TIRF); Spectroscopy of Liquid/Solid Interfaces.

+ Present address: IBM Watson Research Center, Yorktown Heights, NY 10596

INTRODUCTION

The use of fluorescent probe molecules to assess chemical structure and environment is a well established method for investigating biological macromolecules and membranes [1], synthetic polymers [2], vesicles [3], and micelles [4]. In these applications, a particular microchemical environment of the sample selectively binds or adsorbs a fluorescent probe which in turn reports information about its surroundings by its spectroscopic response, including wavelength dependence of its emission and excitation, its excited state lifetime, and emission polarization.

Recently, a number of investigators have used adsorbed or covalently bound fluorescence probes to obtain information about the chemistry of liquid/solid interfaces. In particular, several fluorescence probe studies have addressed the chemistry alkylated silica surfaces, including the proximity of bound ligands [5,6], and the polarity [7-9], heterogeneity [10,11], and microviscosity [12] of the interfacial layer. These investigations have used porous silica as a solid substrate which is advantageous because of its large surface areas (>100 m^2/g), providing large concentrations of surface species and minimizing interferences from the liquid phase. The irregular structure of a porous silica matrix, however, could give rise to a distribution of surface geometries [13] which contribute, in part, to the surface environment and heterogeneity observed in these systems. To ascertain the effects of surface geometry from porous substrates on the chemistry of the solid/liquid interface, we have adapted fluorescent probe methods to optically flat interfaces using total internal reflection fluorescence (TIRF) spectroscopy [14,15]. This development eliminates the influence of the pore structure on the interfacial chemistry so that its effects, if any, might be identified.

TIRF is a spectroscopic technique with surface selectivity based on rapid attenuation of the excitation beam beyond the boundary of a total internal reflection. The method has been applied to a variety of liquid/solid interface studies, including measuring adsorption rates of proteins [16,17], determining the orientation of the fluorophores with respect to the interface by varying the polarization of the excitation beam [18,19], measuring surface diffusion kinetics by correlation methods [20,21] and by photobleaching recovery [22]. By varying the angle of incidence of the excitation beam, the penetration depth of the beam beyond the interface can be controlled. This variation in penetration depth has been used, for example, to study adsorbed protein concentration profiles at interfaces [23]. The technology for obtaining sub-nanosecond time resolution in the gathering of TIRF spectra has also been developed [24,25], creating opportunities for studying interfacial effects on time-dependent phenomena such as fluorescence quenching, energy transfer, and excited state lifetimes.

To utilize fluorescence for studying interfacial molecular environments, a probe molecule, either bound or adsorbed to the solid surface, produces an emission spectrum that is characteristic of its surroundings. To study the polarity of hydrophobic environments, for example, the vibronic band intensities of pyrene are quite sensitive to solvent polarity [26]. As the solvent polarity around pyrene is increased, the intensity of the vibronic origin of the weak, highest energy L_b transition (Band I at 374 nm) is increased due to symmetry lowering perturbations from the solvent environment which allow mixing with the much stronger L_a transition dominating the third vibronic peak (Band III at 385 nm) [27]. As a result, the ratio of the intensities of the third and first peaks, III/I, varies inversely with

increases in the polarity of microenvironment of the pyrene probe [8,26].

The use of pyrene to study interfacial microenvironments of alkylated porous silica by adsorption of the probe to the large area, hydrophobic surface has been demonstrated [8,9,11,12]. To study the interfacial environment of flat, non-porous surfaces, a major challenge in the measurement arises from the small surface area of the interface. The small area limits the number of adsorbed probe molecules that can be observed and greatly increases the magnitude of solution phase interferences. In this study, we assess the potential of total internal reflection to confine the fluorescence excitation to the interfacial region and thus reduce interferences from bulk solution in such measurements. Laser is used for excitation to increase the sensitivity and allow sub-monolayer coverage of probe molecules to be detected. The ratio of vibronic band intensities from the pyrene fluorescence provides a polarity scale of the interface environment. Interference from solution phase probe molecules is modeled using adsorption equilibrium data for the probe and the depth of penetration of the evanescent excitation beam; the model is checked by comparing the probe response at an alkylated silica-solvent vapor interface.

I. EXPERIMENTAL

Total internal reflection fluorimeter. The laser-based, total internal reflection fluorescence instrument used an Innova model 90-K krypton ion laser as an excitation source, operated in the ultraviolet at 351 nm and 365 nm. The 365 nm and interfering plasma lines were eliminated by dispersion through a quartz prism, and all but the 351 nm line of interest were intercepted by a barrier. Additional scattered light was removed by an Ealing interference filter centered at 350 nm with a 10 nm band pass. The excitation beam was passed through a polarization rotator (Special Optics) prior to the cell to rotate the polarization angle by 90° into the of plane incidence to discourage reflections [28] at the coupling between the prism and the fused silica plate (see below). A 50 cm focal length lens was placed in the beam path approximately 1 meter from the cell to provide a beam spot size (radius at $1/e^2$) at the cell of 1.0 mm. Fluorescence was collected with a 5 cm focal length lens, imaged into a 0.2 m Instruments SA monochromator, and detected with a Hamamatsu model R1527 photomultiplier, biased at 900 V. PMT current output was converted to voltage by Keithley model 410 picoammeter and displayed on a strip chart recorder.

The sample cell, shown in Figure 1, was designed to hold an interchangeable, fused silica plate to provide a flat, renewable silica surface for interfacial chemistry studies. One face of this fused silica plate was coupled to a quartz prism to transmit the excitation beam to the silica-solution interface on the other face of the plate (see Figure 2). A brass plate holds the prism and has an opening to allow both passage of the excitation beam and collection of fluorescence emission. The fused silica plate was optically coupled to this prism with a drop of index matching fluid (Cargille 55

immersion fluid, n=1.5320) to discourage reflections at the boundary between them. The opposite face of the fused silica plate was exposed to solutions, confined in a small flow cell volume by a thin silicon rubber gasket. Solutions were introduced into this flow area by threaded inlet and outlet holes in the back plate of the cell assembly. Solvent flow was obtained with a 20 ml syringe driven with a Sage Instruments infusion pump, model 240.

Chemistry. Derivatization of the fused silica plates with octadecylsilane (C-18) surface layer was carried out as follows. Prior to derivatization, the plates were cleaned with chromic acid and concentrated NaOH solution, rinsed with distilled/deionized water, and degreased under freon (1,1,2-trichlorotrifluoroethane, Aldrich) vapor. The clean plates were immersed in a water-saturated toluene solution containing octadecyltrichlorosilane (Aldrich) at a concentration of 2 mM. Coated plates were then rinsed with dry toluene, ethanol, and finally distilled/deionized water. Presence of a C-18 surface layer was confirmed by observing a large contact angles for water on the surface of the plate. The plates were stored in dry air until use.

All solutions were prepared with spectroscopic grade methanol (EM Science), water purified in-house with a Corning still (MP-1) and a Barnstead Nanopure, four-cartridge purification system, and pyrene, used as received from Aldrich. Before each experiment, the test solutions were deoxygenated by sparging with argon gas, saturated with vapor from a large volume solution of the same composition; in this way, the composition of the test solution was not changed. Concentrations of pyrene in the test solutions were optimized to provide suitable signal intensities without the formation of excimer on the plate surface. An effort was made to keep the amount of pyrene adsorbed to the plate constant as solution methanol (MeOH) concentrations were changed. This

was accomplished by varying solution pyrene concentrations inversely with the chromatographic capacity factor, k', for pyrene eluted on a polymeric C18 phase on a porous silica gel support [9]. The pyrene concentrations varied from 5.8 x 10-6 M for 40% MeOH by volume to 2.8 x 10-5 M for 55% MeOH.

Procedures. Following derivatization of the silica plate surface and assembly of the flow cell, one encounters the tedious procedure of adjusting the fluorescence collection optics to assure that emission from pyrene adsorbed to C18 derivatized surface is collected rather than solution phase pyrene excited by scattered excitation radiation and stray reflections. The difficulty of this task was eased by generating a sample having a negligible solution phase pyrene concentration so that optimization of the detected signal is selective for probe molecules on the surface. Such a sample can be prepared by first passing a 55% methanol solution containing pyrene at a concentration of around 30 μM through the cell to allow pyrene to adsorb onto the C18 surface; then the flow is switched from the pyrene-containing solution to pure water. Since the solubility of pyrene in water is quite low, the adsorbed pyrene remains on the hydrophobic surface while the solution phase background from pyrene is virtually eliminated. Translating the collection lens laterally projects regions of varying signal intensity onto the entrance slit of the monochromator, the most intense of which generally corresponds to the optimum zone for detecting the adsorbed pyrene probe. Experience has shown that the signal located in this manner should still be checked for possible solution interference under conditions of the experiment. This can be accomplished by comparing spectra of pyrene solutions prepared with and without an efficient solution phase quencher, such as $Hg(NO_3)_2$ at a concentration of ~50 mM. In such a comparison, a significant solution-phase pyrene interference appears as

a change in both intensity and III/I ratio of the observed fluorescence, as the ionic quencher reduces the intensity of pyrene emission from solution.

For the investigation of the effects of solvent composition, seven spectra were recorded at each composition, to establish the stability of the system and to determine the response of adsorbed pyrene to changes in solvent polarity. Solutions were allowed to flow at least 20 minutes at approximately 0.83 ml/min flow rate before collecting data, in order to equilibrate the composition of the surface-solution interface. As the composition of the solvent was changed, the concentration of pyrene in solution was adjusted in inverse proportion to a chromatographic measurement of the capacity factor k' [9,29] in order to keep the surface concentration of probe molecules constant. Photomultiplier signal currents were consistent with this goal and constantly fell within the range of 10 - 30 nA.

III/I ratios were corrected for the presence of a broad fluorescence background which peaked at approximately 440 nm; the background intensity apparently arose from the fused silica substrate since it did not vary significantly with solvent composition and was not correlated with the presence of pyrene in the solution. A pyrene-free background spectrum was used as a reference, and its intensities at the wavelengths of the first and third vibronic peaks of pyrene, scaled to the peak intensity at 440 nm where pyrene does not emit, were subtracted from the probe spectra before calculating the III/I intensity ratios. Over the range of solvent compositions studied, the maximum relative intensity of this background emission in the vicinity of the vibronic peaks of pyrene was 15% compared to the intensity of the pyrene; thus, the corrections required for the III/I ratios were only slightly larger than the uncertainty in the raw data.

II. RESULTS AND DISCUSSION

Selectivity for Surface Probe Species. The goal of this work is to develop a method to selectively measure fluorescence spectra of adsorbed probe molecules at a solid-liquid interface, while maintaining sufficient spectroscopic resolution to determine the intensity of vibronic bands approximately 10 nm apart. Performance of the total internal reflection fluorescence method proposed to meet this goal is illustrated for pyrene sorbed to a C18 surface in Figure 3, parts b and c, along with spectra in methanol:water solution and a hydrocarbon matrix for comparison in parts a and d, respectively. The vibronic bands are sufficiently resolved to measure III/I ratios, which have been determined from spectra obtained for the pyrene sorbed to the derivatized surface for aqueous solution compositions ranging over 40-55% MeOH by volume. The influence of the solvent on the surface environment is quite apparent in these results, as shown in Figure 4. The solvent dependent changes in surface environment are similar to pyrene sorbed to C18 derivatized porous silica [9], where the polarity of the interface increases (smaller III/I ratio) as the polarity of the overlaying solvent decreases (larger fraction of methanol).

The validity of these results in characterizing the surface environment depends critically on the fraction of signal arising from probe molecules on the surface compared with number excited in the solution adjacent to the interface. While the behavior of the spectroscopic signals indicates that the signal is dominated by adsorbed pyrene, it is useful to check the surface selectivity based on the partition equilibria for pyrene under these conditions and the depth of penetration of the evanescent excitation wave beyond the interface. This surface selectivity depends on the number of sorbed probe molecules per unit surface area compared to the number within the volume of

solvent into which the evanescent wave penetrates.

The fluorescence intensity arising from surface species, $I_{f,s}$, depends on the excitation intensity at the interface, $I_{e,s}$, in photons sec^{-1}, the surface concentration of probe molecules, C_s in molecules per cm^2, the area of the interface illuminated by excitation beam, α, in cm^2, and the fluorescence collection and quantum efficiencies, collected into one term, ξ, where

$$I_{f,s} = \alpha \xi C_s I_{e,s} \quad (1)$$

The excitation beam diameter is 2.0 mm, and produces a 7.5 mm x 2.0 mm illuminated ellipse at the interface having an area of 0.12 cm^2.

If the concentration of probe molecules in bulk solution, C_o in molecules per cm^3, is at equilibrium with a surface concentration of probe molecules, C_s, in a region of linear isotherm behavior, then the mole ratio or capacity factor, k', relates these two concentrations, the surface area, α, and the solution phase volume, Vo, according to [9,30]:

$$C_s = k' V_o C_o/\alpha \quad (2)$$

The surface concentration, thus defined, was estimated from chromatographic retention data [9] gathered on a 10 cm column containing a weighed amount (1.047 g) of ODS-2, a polymeric C18 derivatized porous silica stationary phase from Whatman. From the manufacturer's measurement of the specific surface area of the chromatographic silica, total surface area in the column is calculated to be 1.047 g x (3.20×10^6 cm^2/g) = 3.35×10^6 cm^2. The mobile phase volume of the column was determined to be 0.81 cm^3 [9]. For a specific example calculation of surface concentration, elution of pyrene using an aqueous solution which was 55% by volume methanol resulted in a capacity factor, k'= 1.53×10^2. For this composition of solvent, the concentration of pyrene used

was $C_o = 2.8 \times 10^{-5}$ M or 1.69×10^{16} molecules/cm^3. The resulting surface concentration predicted by Equation 2 is $C_s = 6.3 \times 10^{11}$ molecules/cm^2. Within the excitation area of the laser beam at the interface are N_s molecules at the surface, where $N_s = (C_s \times \alpha) = 7.5 \times 10^{10}$ molecules. Since C_o was varied inversely with k' as the solvent composition was changed, then the number of surface probe molecules are constant (see Equation 2).

The evanescent wave from the reflected excitation beam penetrates the bulk solvent beyond the interface and excites fluorescence from probe molecules in solution. The intensity of background fluorescence from interfering pyrene in bulk solution can be calculated by integrating the fluorescence signal over the excitation intensity distribution beyond the interface:

$$I_{f,b} = \alpha \xi C_o \int_0^\infty I_{e,s} \exp(-2x/d_p)\, dx \qquad (3)$$

where the depth of penetration of the evanescent wave, d_p, is the distance at which the excitation intensity drops by a factor e^{-2} and is given by [28]:

$$d_p = \frac{\lambda}{2\pi n_1 [\sin^2\theta - (n_2/n_1)^2]^{1/2}} \qquad (4)$$

where θ is the angle of incidence (in this case 79.5°), and $n_1 = 1.475$ and $n_2 = 1.34$ are the refractive indices of the fused silica and solvent [31], respectively, at the excitation laser wavelength, $\lambda = 351$ nm. These values lead to a depth of penetration, $d_p = 98$ nm, for these experiments.

For simplicity in Equation 3, the fluorescence collection efficiency has been taken to be independent of distance from the interface and the same as for surface adsorbed species. According to the principle of optical reciprocity [32], this assumption is valid for detecting fluorescence within a collection angle much less than the critical angle where the emission couples to

propagating rather than evanescent modes. The assumption leads to an integral which is simple to evaluate and yields the following expression for the probe fluorescence intensity from bulk solution:

$$I_{f,b} = \alpha \xi I_{e,s} C_o d_p/2 \qquad (5)$$

This expression allows a simple intensity comparison Equation 1 in order to determine the selectivity of the method for surface adsorbed species. The number of probe molecules in bulk solution, detected with equivalent sensitivity as those on the surface, is given by $N_b = (\alpha C_o d_p/2)$; for the 55% methanol conditions ($C_o = 1.69 \times 10^{16}$ molecules/cm^3), $N_b = 9.9 \times 10^9$ molecules.

The selectivity of internal reflection excitation for surface adsorbed probe molecules over those in bulk solution can be characterized by the fraction of background molecules in total number of molecules excited: $N_b/(N_s + N_b) = 12\%$ for 55% methanol conditions. As the concentration of methanol is lowered in the solvent, the capacity factor for the probe, k', is increased due to hydrophobic interactions, the fraction of molecules on the surface is greater. Operationally, to keep the surface concentration of pyrene constant, its solution concentration is lowered in proportion to the increase in k', as described above. The number of surface species remains fixed as predicted by Equation 2, while the number of background pyrene molecules in bulk solution is reduced by a factor 1/k'. With 40% MeOH in the solvent for example, where $k' = 7.3 \times 10^2$, the number of background probe molecules in bulk solution excited by the evanescent wave drops by a factor 5 compared to 55% methanol conditions, and therefore produces a much smaller interference, $N_b/(N_s + N_b) = 2.7\%$.

The surface selectivity results are summarized in Table I for the solvent compositions studied. These results predict the conditions under which the

surface environment can be characterized by an adsorbed fluorescent probe using internal reflection excitation to reduce the sensitivity to bulk probe species. From these predictions, it is evident that the apparent C18 surface environment in contact with 55% MeOH solution reflected in the pyrene III/I ratio is likely to be more polar than the actual surface, since 12% of the signal intensity could arise from solution phase probe molecules. At lower MeOH concentrations, the bulk solution contribution drops rapidly below the relative error in the spectral data and represents an insignificant interference. As a final point, the capacity factor for pyrene, measured chromatographically and listed in Table I, represents a mole ratio of adsorbed to solution phase species in a packed column of C18 porous silica. It is interesting to compare k' to N_s/N_b for the internal reflection experiment, where $k' = 20.2\ N_s/N_b$. This relationship indicates that a slurry-packed column of porous silica has a surface area-to-solution volume ratio which is 20 times greater than surface/solution selectivity of the internal reflection fluorescence experiment. To avoid solution-phase interferences, therefore, the TIRF experiment requires that the affinity of the probe for the surface of interest be 20-times larger than for a comparable study carried out on a packed column of porous silica.

Validity and Interpretation of III/I Vibronic Band Ratios. In order to validate the predictions in Table I concerning interference from solution-phase pyrene emission, a strategy was tested to avoid the problem altogether by eliminating the solvent from the surface in question. Spectra of pyrene sorbed to the C18 surface were gathered with the cell filled with solvent vapor rather than solution. The C18 surface was first equilibrated with a pyrene-containing solution as above, following which air, saturated with the same solvent for

20 min, was admitted to the cell to displace the solvent from the surface. Measurement of the surface environment by this method and its relationship to the liquid-solid interface presumes that solvent components intercalated into the C18 layer during exposure to solution do not change when the solution is replaced by its saturated vapor. This is a reasonable expectation, since an interface layer at equilibrium with a mixed solvent is also at equilibrium with the vapor phase solvent components, each of which is represented in the gas phase at its equilibrium partial pressure at the same temperature.

The III/I vibronic band ratios for pyrene sorbed to a C18 surface in contact with the solvent-saturated vapor are presented in Figure 4, along with the difference in III/I ratios between these results and those from the solution-contacted surface. The systematic increase in the polarity of the surface environment (decreasing III/I ratio) with increasing concentration of methanol is observed under both conditions, similar to the behavior observed in C18 derivatized porous silica [9]. The similar solvent composition dependence of the vapor-contacted surface supports the expectation that the equilibrium distribution of solvent components in the C18 layer is preserved when the solvent is replaced by its saturated vapor at the same temperature. The observed polarity of the vapor-contacted surface is, however, offset from the solution-contacted surface in a direction which indicates that the latter surface is more polar. The amount of the offset is small (~0.25 in the III/I ratio) at the lower concentrations of methanol, but increases nearly linearly as the volume fraction of methanol is raised to 55%. This additional increase in the apparent polarity of the solution-contacted surface is consistent with the growing influence of solution-phase pyrene on the observed signal, as predicted by Table I. At the lower two methanol concentrations,

where the influence of solution-phase background should be negligible, the offset between the two curves is smaller and constant, within the reproducibility of the data.

The residual offset in the apparent polarity of the solution-contacted surface, at lower methanol concentrations, could result from several causes. One contribution could be optical imperfections at the silica-solution interface which allow a small fraction of the excitation radiation to be scattered into bulk solution where it excites solution-phase pyrene. Since the optical path through the flow cell is much larger (x 10^5 times) than the depth of penetration of the evanescent wave, this source of solution-phase background would be expected to dominate at the lowest pyrene concentrations. The significant role of scatter-excited fluorescence at low concentrations of solution-phase fluors has been previously studied by Hlady, Reichert and coworkers [17,33].

A second source of the residual offset, between the solution-contacted and vapor-contacted results, could arise from sorbed pyrene probe being partially exposed to the polar solution in the former case, so that physical removal of the bulk solvent from the interface would lower the apparent polarity of the C18 surface. Indeed, fluorescence quenching by solution-phase ions has been observed for pyrene sorbed to C18 on porous silica at low concentrations of methanol in aqueous solution ($\leq$ 30%) [11]. The III/I ratios for pyrene for the C18 porous silica surfaces (maximum III/I = 1.28) indicate, however, that porous silica substrates generate a much more polar C18 surface than C18 on flat surfaces in the present study. The large values of the III/I ratios shown in Figure 4 are indicative of an environment which perturbs symmetry of highest energy, L_b, transition of pyrene less than a liquid alkane solvent. A

comparison spectrum of pyrene in liquid octadecane (at ca. 50°C) is shown in Figure 3(c), with a III/I ratio of 1.88 (± 0.04). If there were significant exposure of sorbed pyrene to bulk solution in the present results (see Figure 3(a)), then the III/I ratios would be lower not higher than this value.

The extremely low polarity of the C18-derivatized, flat silica surface is a curious and interesting result. This observation is consistent with the C18 chains being symmetrically distributed about the pyrene probe and excluding methanol and water from its environment. A picture emerges of a well organized and ordered array of alkyl chains at the interface, quite different in structure when compared to the same ligands bound to porous silica [9,11,34]. Such a picture would support the description for these monolayers offered by Sagiv [35] of a molecular self-assembly, not unlike Langmuir-Blodgett films. Further investigations of these surfaces with comparisons to similar layers bound to porous silica are currently in progress.

Conclusions. Total internal reflection excitation provides sufficient surface selectivity to allow the environment of the interface to be probed by fluorescent molecules which are adsorbed from solution. With laser excitation, spectra could be obtained using a simple scanning emission monochromator with as few as 2×10^{10} adsorbed fluorescent probe molecules in the excitation beam. Knowledge of the adsorption equilibrium of the probe molecule and the depth of penetration of the evanescent wave beyond the interface permits the range of application of the method to be predicted, where background fluorescence from the probe in bulk solution will be small. As expected on the basis of separated two-phase equilibria, environment of surface monolayers may also be interrogated by replacing overlaying solution with saturated vapor at the same temperature; this procedure appears to maintain the concentration of solvent

constituents in the surface layer established in equilibrium with the solution, and allows solution background to be physically eliminated. Finally, the interfacial environment of C18 alkyl layers on optically flat, fused silica appears to be much more ordered than similar layers bound to porous, particulate silica supports.

ACKNOWLEDGMENTS

The authors express their appreciation to R. Van Wagenen and J. D. Andrade for their help with preliminary experiments. This work was supported in part by the Office of Naval Research.

REFERENCES

1. L. Brand and J. R. Gohlke, Ann. Rev. Biochem. 41, 843 (1972).
2. H. Morawetz, Science, 203, 405 (1979).
3. M. Almgren, J. Amer. Chem. Soc. 102, 7882 (1980).
4. J. K. Thomas, Accts. Chem. Res. 10, 133 (1977).
5. C. H. Lochmüller, A. S. Colborn, M. L. Hunnicutt, and J. M. Harris, Anal. Chem. 55, 1344 (1983).
6. C. H. Lochmüller, A. S. Colborn, M. L. Hunnicutt, and J. M. Harris, J. Amer. Chem. Soc. 106, 4077 (1984).
7. C. H. Lochmüller, D. B. Marshall, and D. R. Wilder, Anal. Chim. Acta 130, 31 (1981).
8. J. Stahlberg, and M. Almgren, Anal. Chem. 57, 817 (1985).
9. J. W. Carr and J. M. Harris, Anal. Chem. 58, 626 (1986).
10. C. H. Lochmüller, D. B. Marshall, and J. M. Harris, Anal. Chim. Acta 131, 263 (1981).
11. J. W. Carr and J. M. Harris, Anal. Chem. 59, 2546 (1987).
12. R. G. Bogar, J. C. Thomas, and J. B. Callis, Anal. Chem. 56, 1080 (1984).
13. D. Avnir, J. Amer. Chem. Soc. 109, 2931 (1987).
14. T. Hirschfeld, Can. Spectrosc. 10, 128 (1965).
15. D. Axelrod, T. P. Burghardt, and N. L. Thompson, Ann. Rev. Biophys. Bioeng. 13, 247 (1984).
16. B.K. Lok, Y.-L. Cheng, and C.R. Robertson, J. Colloid Interface Sci. 91, 87, 104 (1983).
17. V. Hlady, D.R. Reinecke, and J.D. Andrade, J. Colloid Interface Sci. 111, 555 (1986).
18. T.P. Burghardt, J. Chem. Phys. 78, 5913 (1983).

19. N.L. Thompson, H.M. McConnell, and T.P. Burghardt, Biophys. J. 46, 739 (1984).

20. N.L. Thompson and D. Axelrod, Biophys. J. 43, 103 (1983).

21. N.L. Thompson, Biophys. J. 38, 327 (1982).

22. N.L. Thompson, T.P. Burghardt, and D. Axelrod, Biophys. J. 33, 435 (1981).

23. W.M. Reichert, P.A. Suci, J.T. Ives, and J.D. Andrade, Appl. Spectrosc. 41, 503 (1987).

24. H. Masuhara, N. Mataga, S. Tazuke, T. Murao, and I. Yamazaki, Chem. Phys. Lett. 100, 415 (1983).

25. H. Masuhara, S. Tazuke, N. Tamai, and I. Yamazaki, J. Phys. Chem. 90, 5830 (1986).

26. D.C. Dong and M.W. Winnik, Photochem. Photobiol. 35, 17 (1984).

27. F.W. Langkilde, E.W. Thulstrup, and J. Michl, J. Chem. Phys. 78, 3372 (1983).

28. N.J. Harrick. Internal Reflection Spectroscopy. (Wiley Interscience, New York, 1967).

29. J. W. Carr and J. M. Harris, Anal. Chem. 60, 698 (1988).

30. S. Bitteur and R. Rosset, Chromatographia 23, 163 (1987).

31. D. E. Gray, ed., Amer. Inst. Phys. Handbook, 3rd. Ed. (McGraw-Hill, New York, 1972).

32. P.A. Suci and W.M. Reichert, Appl. Spectrosc. 42, 120 (1988).

33. W.M. Reichert, J.T. Ives, P.A. Suci, and V. Hlady, Appl. Spectrosc. 41, 636 (1987).

34. D.R. Wilder and C.H. Lochmüller, J. Chromatogr. Sci. 17, 574 (1979).

35. J. Gun and J. Sagiv, J. Colloid Interface Sci. 112, 457 (1986).

Table I. Background Interference from Pyrene in Solution Phase

% MeOH	k' [a]	N_b (10^9 molecules)	Selectivity (N_S/N_b)	Background Fraction ($N_b/(N_S + N_b)$)
55	153	9.9	7.6	12 %
50	240	6.1	12	7.5 %
45	420	3.5	21	4.5 %
40	730	2.1	36	2.7 %

[a] For chromatographic elution; data from Reference 9.

FIGURE CAPTIONS

1. Three-dimensional view of TIRF cell showing: A) opening in front plate for entrance of excitation beam and collection of fluorescence radiation, B) front brass plate, C) total internal reflection prism, D) fused silica plate, E) silastic gasket, F) anodized aluminum cover plate, and G) aluminum back plate.
2. Cross-sectional view of TIRF cell showing: A) excitation laser beam path, B) front brass plate, C) total internal reflection prism, D) fused silica plate, E) silastic gasket, F) anodized aluminum cover plate, G) aluminum back plate, H) solvent flow path through aluminum plates and gasket opening, and I) emitted fluorescence from the interface.
3. Illustration of spectra from pyrene in various environments. Labeled are the specific vibronic bands of interest in the study: III (385 nm), and I (374 nm). A) Solution phase (65% MeOH) pyrene spectrum obtained with the TIRF instrument set-up with an underivatized, non-adsorbing fused silica plate present in the flow cell. B,C) Two adsorbed pyrene spectra obtained with and without overlaying solution (50% MeOH) in the cell, respectively. D) Spectrum of pyrene dissolved in liquid octadecane, for comparison.
4. Plot of Pyrene III/I ratio vs. % MeOH for solution (triangles) and vapor (squares) filled cell, along with the calculated offset between the two (circles).

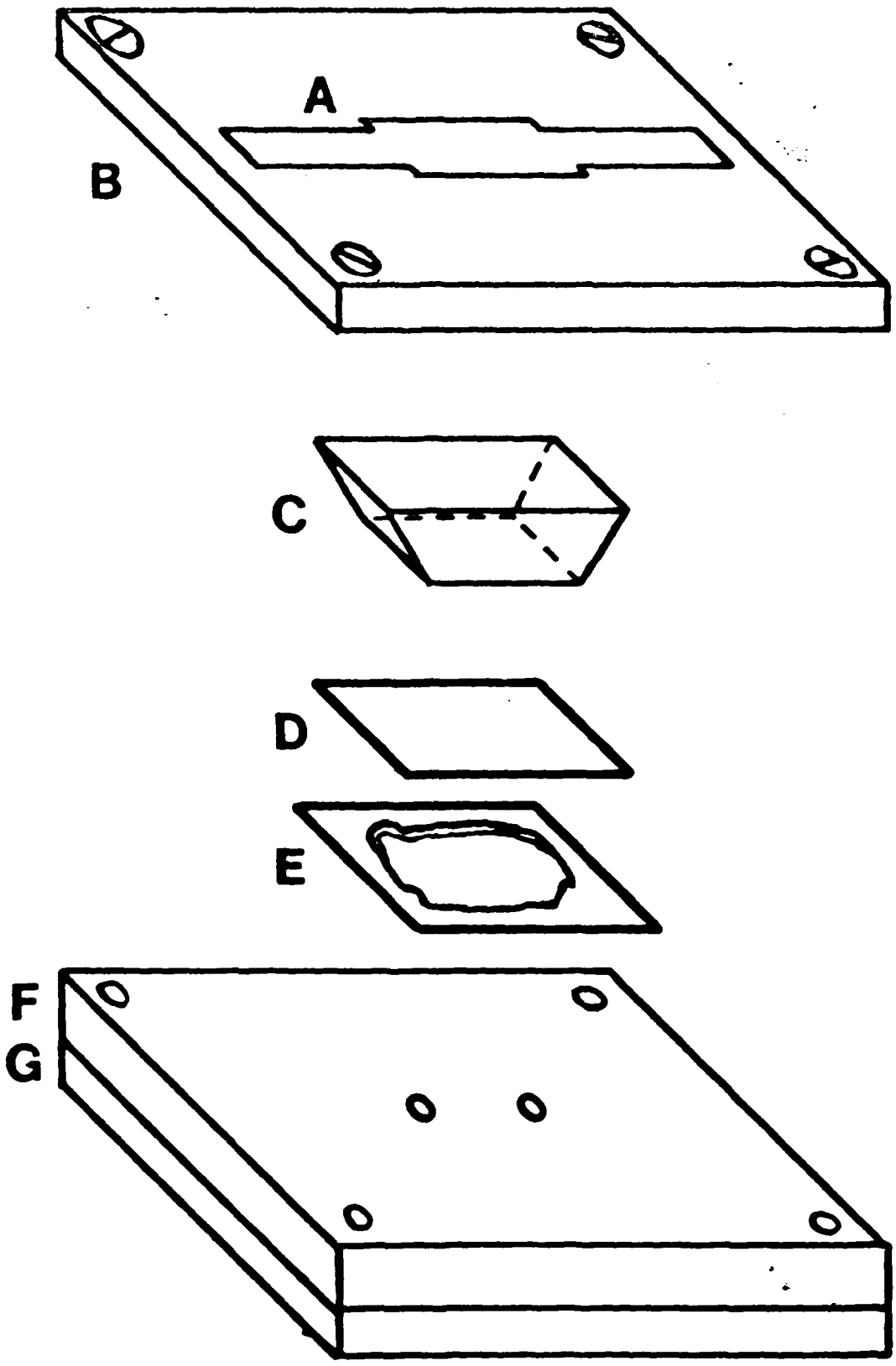

Fig 1

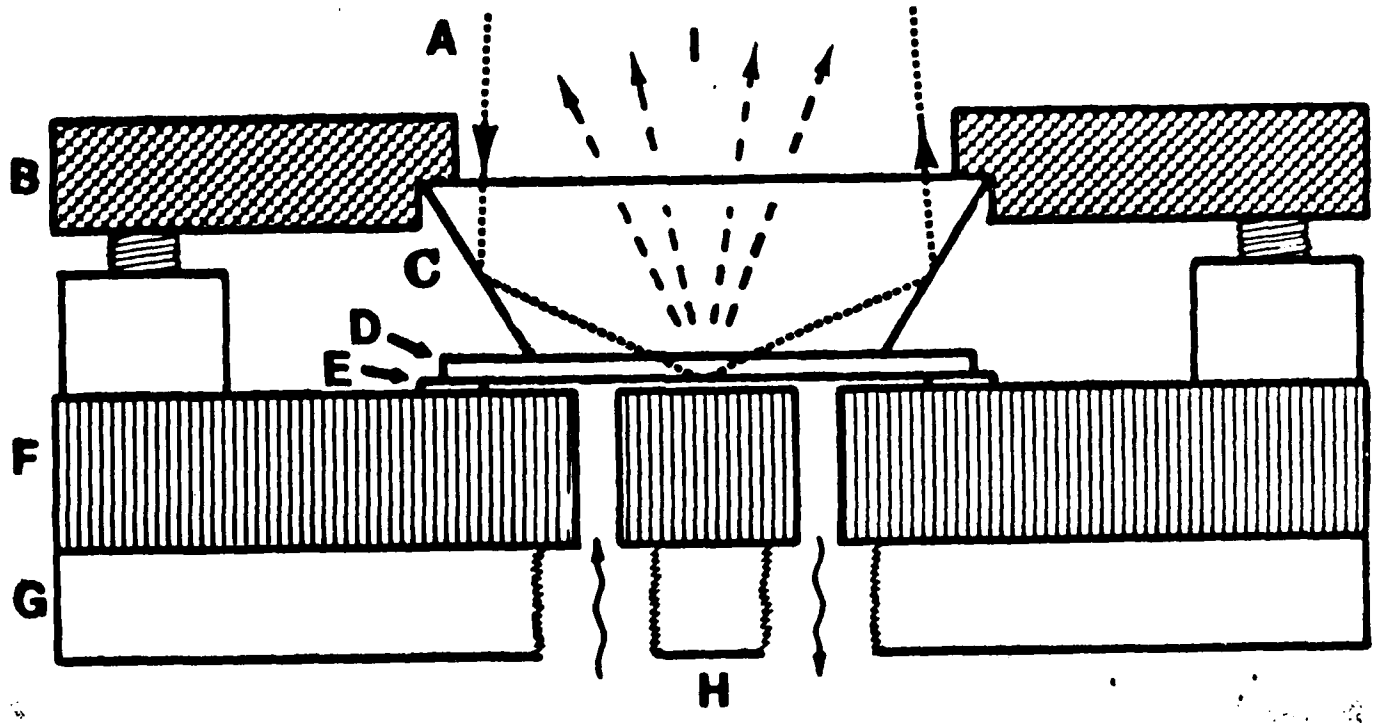

Fig 2

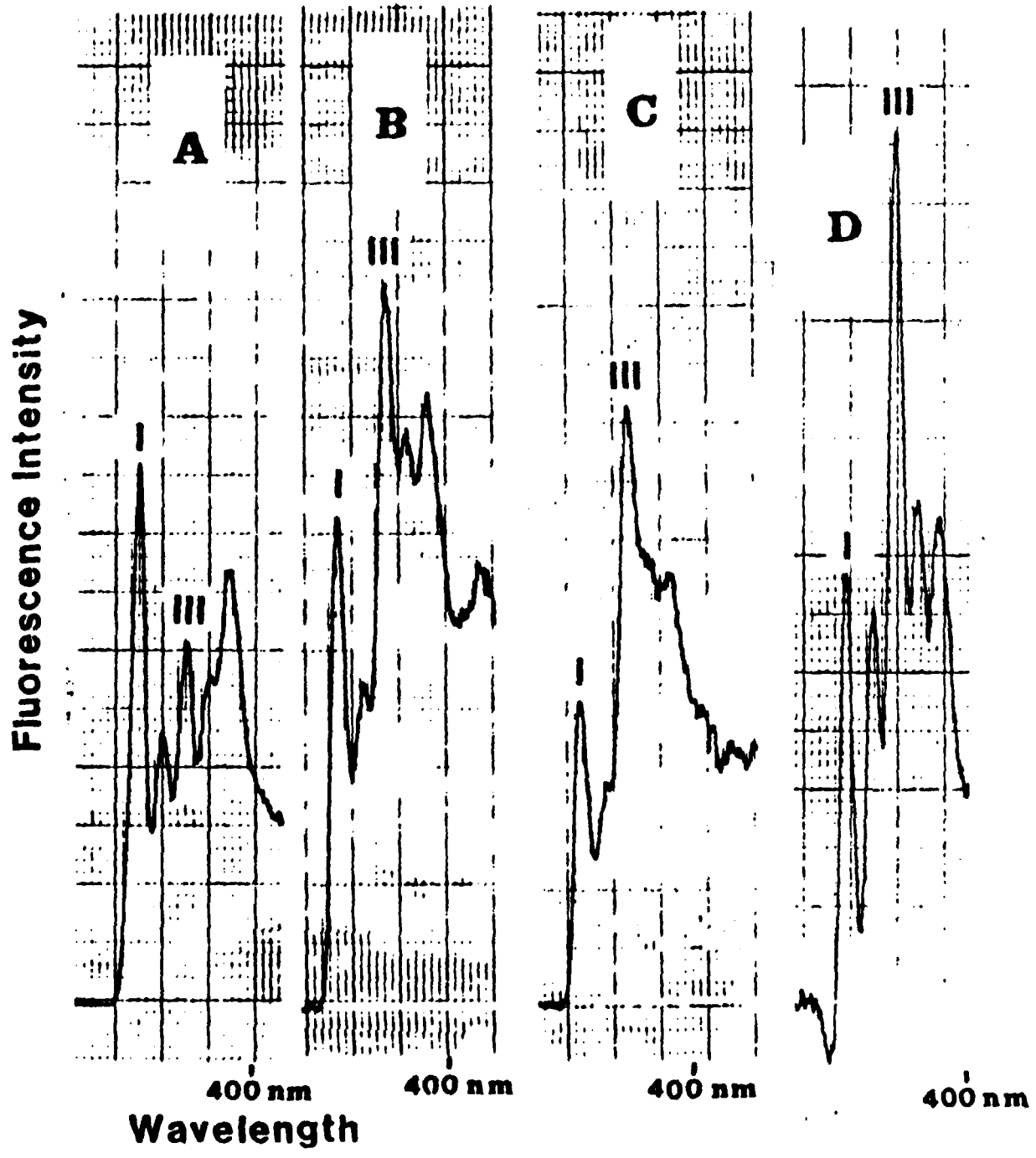
A
B
C
D
I
II
III
Fluorescence Intensity
400 nm
400 nm
400 nm
400 nm
Wavelength

Fig. 3

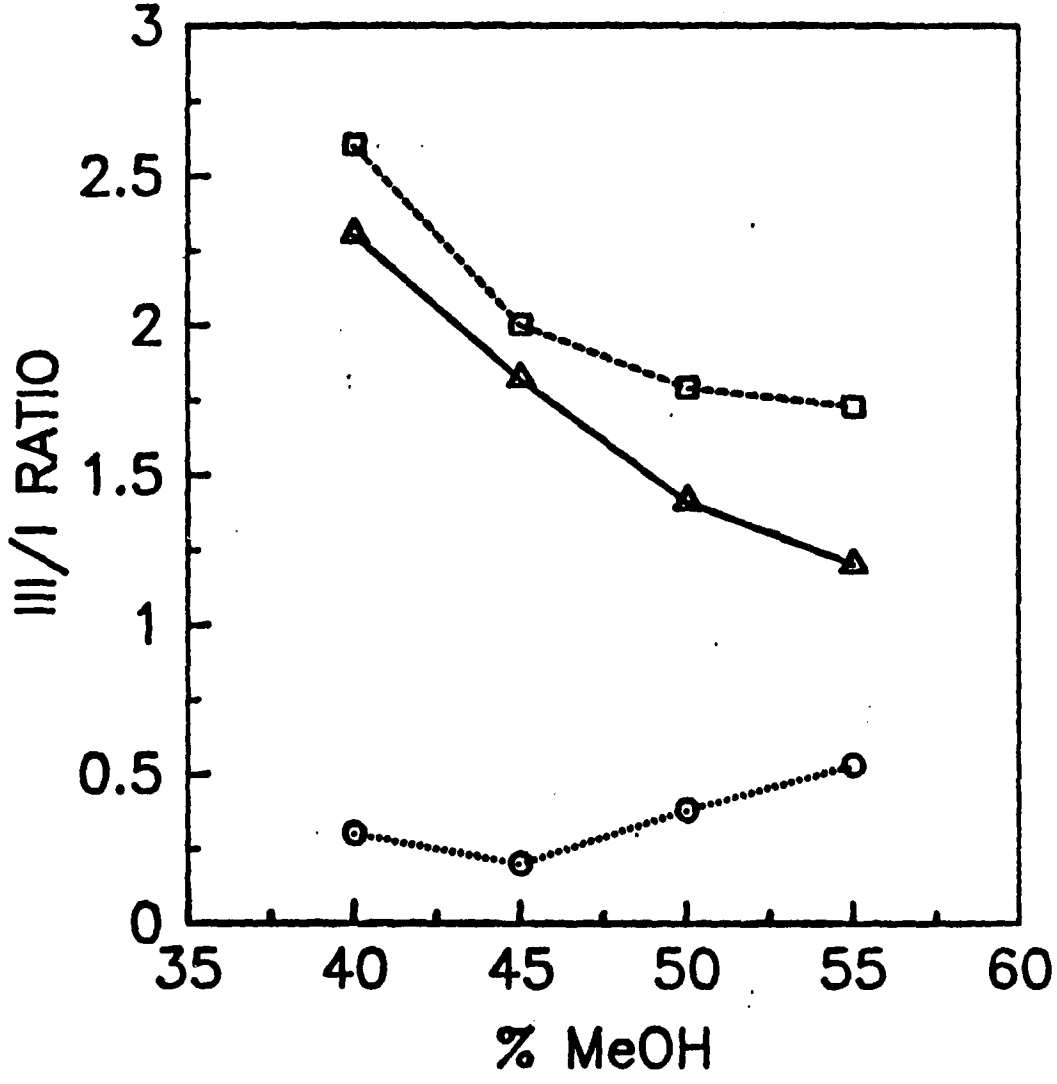

Fig.4